

Configuration mixings and light-front relativistic quark model predictions for the electroexcitation of the $\Delta(1232)_{\frac{3}{2}}^{+}$, $N(1440)_{\frac{1}{2}}^{+}$, and $\Delta(1600)_{\frac{3}{2}}^{+}$

I.G. Aznauryan^{1,2} and V.D. Burkert¹

¹ Thomas Jefferson National Accelerator Facility, Newport News, Virginia 23606, USA

² Yerevan Physics Institute, 375036 Yerevan, Armenia

We investigate the impact of the configurations mixings that follow from QCD-inspired interquark forces on our results for the electroexcitation of the $\Delta(1232)_{\frac{3}{2}}^{+}$, $N(1440)_{\frac{1}{2}}^{+}$, and $\Delta(1600)_{\frac{3}{2}}^{+}$ obtained earlier in the light-front relativistic quark model. We have shown that the configurations mixings increase the $3q$ contribution to the $\gamma^*N \rightarrow \Delta(1232)_{\frac{3}{2}}^{+}$ magnetic-dipole form factor at $Q^2 = 0$ from 42% to 63% and significantly improve the agreement with experiment for the $\gamma^*p \rightarrow N(1440)_{\frac{1}{2}}^{+}$ transverse helicity amplitude at $Q^2 > 1.5$ GeV². For the $\gamma^*N \rightarrow \Delta(1600)_{\frac{3}{2}}^{+}$ transition, configuration mixings change strongly the results obtained earlier for the N and $\Delta(1600)_{\frac{3}{2}}^{+}$ taken as pure states in the multiplets $[56, 0^+]$ and $[56', 0^+]$.

PACS numbers: 12.39.Ki, 13.40.Gp, 13.40.Hq, 14.20.Gk

I. INTRODUCTION

Recently we have reported light-front relativistic quark model (LF RQM) predictions for the $\gamma^*N \rightarrow N$ form factors and the $\gamma^*N \rightarrow \Delta(1232)_{\frac{3}{2}}^{+}$, $N(1440)_{\frac{1}{2}}^{+}$, and $\Delta(1600)_{\frac{3}{2}}^{+}$ transitions [1, 2]. The predictions were made assuming that the N and $\Delta(1232)_{\frac{3}{2}}^{+}$ are pure states in the multiplet $[56, 0^+]$, and the $N(1440)_{\frac{1}{2}}^{+}$ and $\Delta(1600)_{\frac{3}{2}}^{+}$ are members of the multiplet $[56', 0^+]$. However, it is known that in the QCD inspired quark models, where the unknown long-distance properties of QCD are subsumed into a confining potential, the remaining interquark forces are assumed to be dominated by the one-gluon exchange [3–6]. These interquark forces result in configuration mixings. In a space corresponding to the $SU(6)$ multiplets [56], [70], and [20], the mixings have been investigated in Refs. [4–6], and it was found that the N , $\Delta(1232)_{\frac{3}{2}}^{+}$, $N(1440)_{\frac{1}{2}}^{+}$, and $\Delta(1600)_{\frac{3}{2}}^{+}$ are predominantly mixings of the states $[56, 0^+]$, $[56', 0^+]$, and $[70, 0^+]$:

$$|X, 3q\rangle = a_X[56, 0^+] + b_X[56', 0^+] + c_X[70, 0^+], \quad (1)$$

$$|X_r, 3q\rangle = a_{X_r}[56', 0^+] + b_{X_r}[56, 0^+] + c_{X_r}[70, 0^+], \quad (2)$$

where X and X_r denote, respectively, the N , $\Delta(1232)_{\frac{3}{2}}^{+}$ and the $N(1440)_{\frac{1}{2}}^{+}$, $\Delta(1600)_{\frac{3}{2}}^{+}$. With this, $c_\Delta = c_{\Delta_r} = 0$, and the coefficients in the expansions of Eqs. (1,2) are correlated with each other:

$$b_N \simeq -b_\Delta \simeq -b_{N_r} \simeq b_{\Delta_r} < 0, \quad (3)$$

$$c_N \simeq -c_{N_r} \simeq b_N < 0. \quad (4)$$

Absolute values of coefficients in Eqs. (3,4) are ~ 0.22 in Refs. [4, 5] and ~ 0.29 in Ref. [6]. The coefficients a_X are respectively: $a_N \simeq a_{N_r} \simeq 0.95$, $a_\Delta \simeq a_{\Delta_r} \simeq 0.97$ and $a_N \simeq a_{N_r} \simeq 0.91$, $a_\Delta \simeq a_{\Delta_r} \simeq 0.96$.

In this note we present our results for the $\gamma^*N \rightarrow \Delta(1232)_{\frac{3}{2}}^{+}$, $N(1440)_{\frac{1}{2}}^{+}$, and $\Delta(1600)_{\frac{3}{2}}^{+}$ transitions ob-

tained within LF RQM taking into account the configuration mixings from Eqs. (1-4). The results are presented in Sections II, III, IV and summarized in Sec. V.

II. THE $\Delta(1232)_{\frac{3}{2}}^{+}$ RESONANCE

The role of the states $[56', 0^+]$ and $[70, 0^+]$ in the description of the $\gamma^*N \rightarrow N$ and $\gamma^*N \rightarrow \Delta(1232)_{\frac{3}{2}}^{+}$ form factors has been considered and presented in very detail in Ref. [7]. It was shown that with the relations of Eqs. (3,4), the summary contribution of higher excitation states to nucleon form factors leads to results that are equivalent to the results for the pure $[56, 0^+]$ state at a different value of the parameter α in the radial part of the wave functions:

$$\Phi \sim \exp(-M_0^2/6\alpha^2), \quad (5)$$

where M_0 is the invariant mass of three quarks. More specifically, calculations show that the results for the nucleon form factors obtained in Ref. [1] for the nucleon as pure $[56, 0^+]$ state with $\alpha = 0.37$ GeV are reproduced for the nucleon from Eq. (1) with $\alpha = 0.33$ and 0.32 GeV for the configuration mixings from Refs. [4, 5] and [6], respectively.

The states from $[56', 0^+]$ do not contribute to the $\gamma^*N \rightarrow \Delta(1232)_{\frac{3}{2}}^{+}$ transition because $b_N \simeq -b_\Delta$ (see Eq. (3)), and the state $\frac{1}{2}^{+}$ from $[70, 0^+]$ gives negligible contribution to this transition. Therefore, for $\gamma^*N \rightarrow \Delta(1232)_{\frac{3}{2}}^{+}$ the difference in the LF RQM predictions, caused by the admixtures of higher excitation states in the N and $\Delta(1232)_{\frac{3}{2}}^{+}$, is determined only by the replacement $\alpha = 0.37 \rightarrow 0.32$ (or 0.33) GeV.

The predictions for the $\gamma^*N \rightarrow N$ form factors and the $\gamma^*N \rightarrow \Delta(1232)_{\frac{3}{2}}^{+}$ and $\gamma^*N \rightarrow N(1440)_{\frac{1}{2}}^{+}$ transitions were made in Refs. [1, 2] under the assumption that in addition to the three-quark (3q) contribution,

these transitions contain contributions, which are produced by meson-baryon interaction. The nucleon electromagnetic form factors were described by combining $3q$ and pion-nucleon loops contributions. With the pion-nucleon loops evaluated according to the LF approach of Ref. [8], the following form of the nucleon wave function has been found:

$$|N\rangle = 0.95|3q\rangle + 0.313|\pi N\rangle. \quad (6)$$

For the $\Delta(1232)\frac{3}{2}^+$ and $N(1440)\frac{1}{2}^+$, the weights of the $|3q\rangle$ component in the expansion

$$|X\rangle = c_{3q}(X)|3q\rangle + \dots \quad (7)$$

were found from experimental data on the $\gamma^*N \rightarrow \Delta(1232)\frac{3}{2}^+$ and $\gamma^*N \rightarrow N(1440)\frac{1}{2}^+$ transitions assuming that at $Q^2 > 4 \text{ GeV}^2$ these transitions are determined only by the first term in Eq. (7).

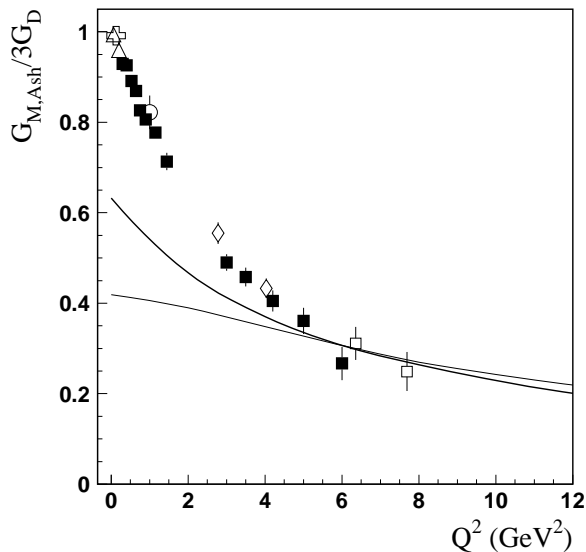


FIG. 1: The form factor $G_{M,Ash}(Q^2)$ for the $\gamma^*p \rightarrow \Delta(1232)\frac{3}{2}^+$ transition relative to $3G_D$: $G_D(Q^2) = 1/(1 + \frac{Q^2}{0.71 \text{ GeV}^2})$. The full boxes are the CLAS data extracted in the analysis of Ref. [10]. The results from other experiments are: open boxes [15], open triangles [17–19], open cross [20–22], open rhombuses [23], and open circle [24, 25]. The thin solid curve presents the LF RQM predictions from Ref. [2] obtained for the N and $\Delta(1232)\frac{3}{2}^+$ taken as pure states in the multiplet $[56, 0^+]$. The thick solid curve corresponds to the LF RQM results when the admixtures of higher excitation states in the N and $\Delta(1232)\frac{3}{2}^+$ are taken into account with the weights from Refs. [4–6].

The predictions for the magnetic-dipole $\gamma^*p \rightarrow \Delta(1232)\frac{3}{2}^+$ form factor in the Ash convention [9] are presented in Fig. 1. In the case, when the N and $\Delta(1232)\frac{3}{2}^+$ are pure $[56, 0^+]$ states, the predictions are given by the thin solid curve; they coincide with the results of Ref. [2].

The thick solid curve corresponds to the results when the admixtures of higher excitation states in the N and $\Delta(1232)\frac{3}{2}^+$ are taken into account. These admixtures increase the $3q$ contribution to the $\gamma^*N \rightarrow \Delta(1232)\frac{3}{2}^+$ magnetic-dipole form factor at $Q^2 = 0$ from 42% to 63%. The weight of the $|3q\rangle$ component in the $\Delta(1232)\frac{3}{2}^+$ is, respectively, $c_{3q}(\Delta) = 0.84 \pm 0.04$ and $c_{3q}(\Delta) = 0.91 \pm 0.04$ for the admixtures of higher excitation states from Refs. [4, 5] and [6].

We note, that both predictions for the $3q$ contribution to the $\gamma^*N \rightarrow \Delta(1232)\frac{3}{2}^+$ magnetic-dipole form factor are within limits obtained in the dynamical reaction model [26, 27], where the bare contribution, that can be associated with the $3q$ contribution, gives at $Q^2 = 0$ about 40–70% of the total magnetic-dipole form factor.

For the ratios R_{EM} and R_{SM} , the admixtures of higher excitation states in the N and $\Delta(1232)\frac{3}{2}^+$, do not affect the results obtained in Ref. [2].

III. THE $N(1440)\frac{1}{2}^+$ RESONANCE

Similar to the electroexcitation of the $\Delta(1232)\frac{3}{2}^+$, the second terms in the expansions of Eqs. (1,2) do not contribute to the $\gamma^*N \rightarrow N(1440)\frac{1}{2}^+$ transition because $b_N \simeq -b_{N_r}$. In addition, the states from $[70, 0^+]$ give negligible contribution to this transition. Therefore, for $\gamma^*N \rightarrow N(1440)\frac{1}{2}^+$ too, the difference in the LF RQM predictions, caused by the configuration mixings, is determined only by the replacement $\alpha = 0.37 \rightarrow 0.32$ (or 0.33) GeV.

The predictions for the $\gamma^*N \rightarrow N(1440)\frac{1}{2}^+$ helicity amplitudes are presented in Fig. 2. In the case, when the N and $N(1440)\frac{1}{2}^+$ are pure states in $[56, 0^+]$ and $[56', 0^+]$, the predictions are given by the thin solid curves; they coincide with the results of Ref. [1].

The thick solid curves correspond to the results when configuration mixings in the N and $N(1440)\frac{1}{2}^+$ are taken into account. These mixings clearly improve the agreement with experiment for the transverse $A_{1/2}$ amplitude above 1.5 GeV^2 , while the behavior of this amplitude below 0.6 GeV^2 remains unchanged. The weight of the $|3q\rangle$ component in the $N(1440)\frac{1}{2}^+$ is, respectively, $c_{3q}(N_r) = 0.91 \pm 0.05$ and $c_{3q}(N_r) = 0.95 \pm 0.05$ with the configuration mixings from Refs. [4, 5] and [6].

In Fig. 2, we also present the predictions obtained within DSE's in QCD [13, 14], which allow most direct connection between quark-quark interaction of QCD and hadron observables. We note remarkable agreement between Q^2 dependences of the transverse amplitude $A_{1/2}$ obtained within DSE's and in the LF RQM with configuration mixings taken into account.

IV. THE $\Delta(1600)\frac{3}{2}^+$ RESONANCE

In contrast with the $\Delta(1232)\frac{3}{2}^+$ and $N(1440)\frac{1}{2}^+$, configuration mixings have a very strong impact on the results for the $\Delta(1600)\frac{3}{2}^+$. The reasons are following:

(1) The contribution to $\gamma^*N \rightarrow \Delta(1600)\frac{3}{2}^+$ corresponding to the unmixed $|N, 3q \rangle = [56, 0^+]$ and $|\Delta_r, 3q \rangle = [56', 0^+]$ is suppressed compared to the contributions from the transitions between $|N, 3q \rangle = [56, 0^+]$ and $|\Delta_r, 3q \rangle = [56, 0^+]$, and $|N, 3q \rangle = [56', 0^+]$ and $|\Delta_r, 3q \rangle = [56', 0^+]$. For example, for the helicity amplitudes in the units of $10^{-3}\text{GeV}^{-1/2}$ at $Q^2 = 0$ we have:

$$A_{1/2} = -49.7(1 + 3.9a_{\Delta_r}b_N + 4.3a_Nb_{\Delta_r}), \quad (8)$$

$$A_{3/2} = -54.6(1 + 5.9a_{\Delta_r}b_N + 6.4a_Nb_{\Delta_r}), \quad (9)$$

$$S_{1/2} = -16.8(1 + 4.8a_{\Delta_r}b_N + 5.5a_Nb_{\Delta_r}). \quad (10)$$

In addition, in contrast with the $N(1440)\frac{1}{2}^+$, for the $\Delta(1600)\frac{3}{2}^+$ we have $b_N \simeq b_{\Delta_r}$ (see Eq. (3)).

From Eqs. (8-10), it follows that at $Q^2 = 0$ the $\gamma^*N \rightarrow \Delta(1600)\frac{3}{2}^+$ helicity amplitudes change their sign. With increasing Q^2 , the relative values of the contributions caused by the configuration mixings become smaller, and the $\gamma^*N \rightarrow \Delta(1600)\frac{3}{2}^+$ amplitudes don't change sign.

(2) For the reasons given in point (1), the additional sign in the helicity amplitudes related to the $\pi N \Delta(1600)\frac{3}{2}^+$ vertex is changing. Let us remind, that this sign has been found in Refs. [2, 30] in the approach based on partial conservation of axial current (PCAC) and is determined by the expression:

$$I_{NA} \equiv \int \frac{(m_q + M_0 x_a)^2 - \mathbf{q}_{a\perp}^2}{(m_q + M_0 x_a)^2 + \mathbf{q}_{a\perp}^2} \Phi_N(M_0^2) \Phi_A(M_0^2) d\Gamma, \quad (11)$$

where A denotes the states N , $\Delta(1232)\frac{3}{2}^+$, $N(1440)\frac{1}{2}^+$, and $\Delta(1600)\frac{3}{2}^+$. In Eq. (11), m_q is the constituent quark mass, x_a is the fraction of the initial nucleon momentum carried by the active quark, $\mathbf{q}_{a\perp}$ is the transverse momentum of this quark, and $d\Gamma$ is the phase space volume of the quarks. These quantities are defined in more detail in Refs. [2, 30]. For the reasons mentioned in point (1), the expression in Eq. (11) changes its sign for the $\Delta(1600)\frac{3}{2}^+$, while for the N , $\Delta(1232)\frac{3}{2}^+$, and $N(1440)\frac{1}{2}^+$ its sign remains unchanged. Therefore, finally at $Q^2 = 0$ the $\gamma^*N \rightarrow \Delta(1600)\frac{3}{2}^+$ helicity ampli-

tudes change their sign twice and remain negative. At large Q^2 , these amplitudes change their sign once. The Q^2 evolution of the predictions for the helicity amplitudes is given in Fig. 3.

V. SUMMARY

We have shown that the configurations mixings which follow from QCD-inspired interquark forces with the weights found in Refs. [4–6] have significant impact on the LF RQM predictions for the electroexcitation of the $\Delta(1232)\frac{3}{2}^+$ and $N(1440)\frac{1}{2}^+$, and result in qualitative changes of the helicity amplitudes predicted for the $\gamma^*N \rightarrow \Delta(1600)\frac{3}{2}^+$ transition.

For the $\Delta(1232)\frac{3}{2}^+$, the admixtures of higher excitation states in the N and $\Delta(1232)\frac{3}{2}^+$ increase the $3q$ contribution to the $\gamma^*N \rightarrow \Delta(1232)\frac{3}{2}^+$ magnetic-dipole form factor, in particular at $Q^2 = 0$, the $3q$ contribution to this form factor grows from 42% to 63%. The predictions for the ratios R_{EM} and R_{SM} remain unchanged.

For the $N(1440)\frac{1}{2}^+$, incorporating the configuration mixings in the N and $N(1440)\frac{1}{2}^+$ leads to better agreement with experiment for the transverse helicity amplitude above 1.5 GeV². The predictions for this amplitude below 0.6 GeV², including zero-crossing at $Q^2 \simeq 0.1$ GeV², remain unchanged.

For the $\Delta(1600)\frac{3}{2}^+$, the specific behavior of the transverse helicity amplitudes with zero-crossing near $Q^2 = 0.2$ GeV², obtained earlier for the pure N and $\Delta(1600)\frac{3}{2}^+$ from the multiplets $[56, 0^+]$ and $[56', 0^+]$, disappears when configuration mixings in these states are taken into account. The configuration mixings result also in the change of the additional sign related to the $\pi N \Delta(1600)\frac{3}{2}^+$ vertex. As a result, both transverse amplitudes become negative at all Q^2 with absolute values that slowly decrease with increasing Q^2 .

Acknowledgments. We are grateful to C. Roberts and V. Mokeev for useful correspondence. This work was supported by the U.S. Department of Energy, Office of Science, Office of Nuclear Physics, under Contract No. DE-AC05-06OR23177, and the National Science Foundation, State Committee of Science of the Republic of Armenia, Grant No. 15T-1C223.

[1] I. G. Aznauryan and V. D. Burkert, Phys. Rev. C **85**, 055202 (2012).
[2] I. G. Aznauryan and V. D. Burkert, Phys. Rev. C **92**, 035211 (2015).
[3] A. De Rujula, H. Georgi, and S. L. Glashow, Phys. Rev. D **12**, 147 (1975).

[4] S. S. Gershtein and G. V. Dzhikha, Yad. Fiz. **34**, 1566 (1981).
[5] N. Isgur, G. Karl, and R. Koniuk, Phys. Rev. D **25**, 2394 (1982).
[6] N. Isgur, G. Karl, and J. Soffer, Phys. Rev. D **35**, 1665 (1987).

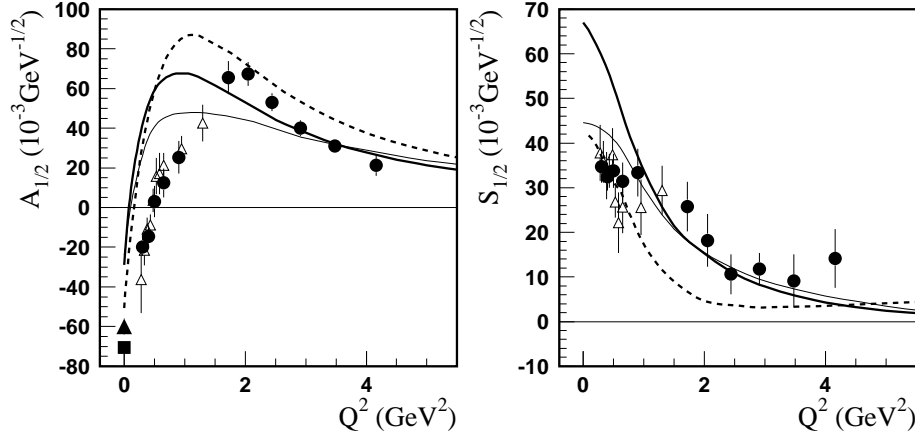


FIG. 2: The $\gamma^* p \rightarrow N(1440)\frac{1}{2}^+$ transition helicity amplitudes. Solid circles and open triangles are the amplitudes extracted from the CLAS data on πN [10] and $\pi^+ \pi^- p$ [11, 12] electroproduction off the proton. The full box at $Q^2 = 0$ is the amplitude extracted from the CLAS π photoproduction data [28]. The full triangle at $Q^2 = 0$ is the Review of Particle Physics (RPP) estimate [29]. The thin solid curves present the LF RQM predictions from Ref. [1] obtained for the N and $N(1440)\frac{1}{2}^+$ taken as pure states in the multiplets $[56, 0^+]$ and $[56', 0^+]$. The thick solid curves correspond to the LF RQM results when the configuration mixings in the N and $N(1440)\frac{1}{2}^+$ are taken into account with the weights from Refs. [4–6]. The dashed curves are the results obtained within Dyson-Schwinger equations (DSE) in QCD [13, 14].

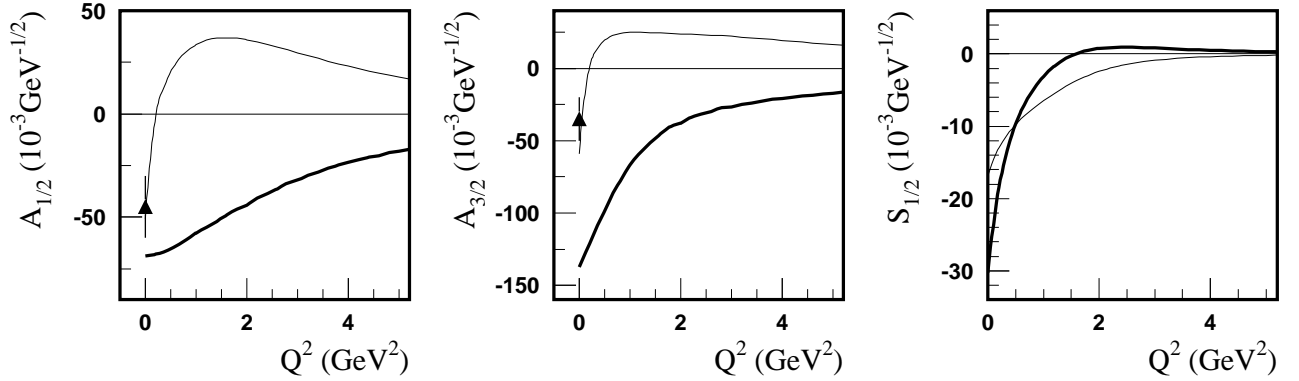


FIG. 3: Helicity amplitudes for the $\gamma^* p \rightarrow \Delta(1600)\frac{3}{2}^+$ transition. The full triangles at $Q^2 = 0$ are the RPP estimates [29]. The thin solid curves present the LF RQM predictions when the N and $\Delta(1600)\frac{3}{2}^+$ are pure states from the multiplets $[56, 0^+]$ and $[56', 0^+]$. The thick solid curves correspond to the results when the configuration mixings in the N and $\Delta(1600)\frac{3}{2}^+$ are taken into account with the weights from Refs. [4–6].

- [7] I. G. Aznauryan, Z. Phys. A **346**, 297 (1993).
- [8] G. A. Miller, Phys. Rev. C **66**, 032201 (2002).
- [9] W.W. Ash, Phys. Lett. B **24**, 165 (1967).
- [10] I. G. Aznauryan et al., CLAS Collaboration, Phys. Rev. C **80**, 055203 (2009).
- [11] V. I. Mokeev et al., CLAS Collaboration, Phys. Rev. C **86**, 035203 (2012).
- [12] V. I. Mokeev et al., CLAS Collaboration, Phys. Rev. C **93**, 025206 (2016).
- [13] J. Segovia, B. El-Bennich, E. Rojas et al., Phys. Rev. Lett. **115**, 171801 (2015).
- [14] C. D. Roberts and J. Segovia, arXiv:1603.02722 [nucl-th].
- [15] A.N. Villano et al., Phys. Rev. C **80**, 035203 (2009).
- [16] I. G. Aznauryan, V. D. Burkert, Prog. Part. Nucl. Phys. **67**, 1 (2012), arXiv:1109.1720, 2011.
- [17] S. Stave et al., Eur. Phys. J. A **30**, 471 (2006).
- [18] N.F. Sparveris et al., Phys. Lett. B **651**, 102 (2007).
- [19] S. Stave et al., Phys. Rev. C **78**, 025209 (2008).
- [20] C. Mertz et al., Phys. Rev. Lett. **86**, 2963 (2001).
- [21] C. Kunz et al., Phys. Lett. B **564**, 21 (2003).
- [22] N.F. Sparveris et al., Phys. Rev. Lett. **94**, 022003 (2005).
- [23] V.V. Frolov et al., Phys. Rev. Lett. **82**, 45 (1999).
- [24] J. J. Kelly et al., Phys. Rev. Lett. **95**, 102001 (2005).
- [25] J. J. Kelly et al., Phys. Rev. C **75**, 025201 (2007).
- [26] T. Sato and T.-S. H. Lee, Phys. Rev. C **63**, 055201 (2001).
- [27] B. Julia-Diaz, T.-S. H. Lee, A. Matsuyama, T. Sato, and L. C. Smith, Phys. Rev. C **77**, 045205 (2008).
- [28] M. Dugger et al., CLAS Collaboration, Phys. Rev. C **79**, 065206 (2009).
- [29] K. A. Olive et al., Chin. Phys. C **38**, 090001 (2014).
- [30] I. G. Aznauryan, Phys. Rev. C **76**, 025212 (2007).